Negative Pion Induced Reactions in Bismuth at 0.87 GeV

Tomota Nishi,* Ichiro Fujiwara,* Nobutsugu Imanishi,* Hirotake Moriyama,**
Kiyoteru Otozai,*** Ryuichi Arakawa,**** Tadashi Saito,****
Toshihiro Tsuneyoshi,**** Narito Takahashi,**** Shiro Iwata,*****
Shigeki Hayashi,***** Seiichi Shibata,******
Hisaaki Kudo,******* and Kunio Yoshida********

Cross sections of more than forty radioactive products have been measured for the negative pion induced reactions in bismuth at 0.87 GeV. Many of the radionuclides were measured by direct γ-ray spectroscopy of the irradiated targets; the yields of the deep spallation and the binary fission products were measured after the radiochemical separations. The mass yield curve was derived by using the estimated charge dispersion curves. General trends of pion induced reactions such as the slope of mass yield curve (~7%/amu) show a good accordance with those of the proton induced reactions. However, the estimated binary fission cross section of ~50 mb is considerably lower than that reported for 1 GeV p+Bi.

I. INTRODUCTION

The interactions of pions with complex nuclei have been the subject of a number of publications.[1~7] Those studies, most of which concentrated on reactions with light nuclei (A<70), have shown some different featues from the proton induced reactions, indicating the importance of the pion-nucleon resonances. However, further studies with heavy nuclei seem desirable, which will provide additional tests for the conclusions concerning the difference between the pion and the proton induced reactions.

In the present study, yields of more than forty nuclides from the interactions of 0.87 GeV π^- with bismuth were measured. Yield patterns deduced by constructing mass-yield curve are compared with the other experimental and the calculated ones. Binary fission cross section was also measured and compared with those of proton induced reactions in Bi, Th, and U.[8~10]

西　朋太，藤原一郎，今西信嗣，森山裕丈，音在清輝，荒川隆一，斉藤　直，常吉俊宏，高橋
成人，岩田志郎，林　茂樹，柴田誠一，工藤久昭，吉田邦夫
　　* Institute of Atomic Energy, Kyoto Univerity, Uji, Kyoto, 611.
　　** Faculty of Engineering, Kyoto University, Kyoto 606.
　*** Kobe Womens' University, Suma, Kobe 654.
　**** Faculty of Science, Osaka University, Osaka 560.
　***** Research Reactor Institute, Kyoto University, Kumatori, Osaka 590-04.
　****** Institute for Nuclear Study, University of Tokyo, Tanashi, Tokyo 188.
　******* Faculty of Science, Tokyo Metropolitan University, Tokyo 158.
******** Institute for Solid State Physics, University of Tokyo, Tokyo 106.

II. EXPERIMENTAL

Irradiations at 0.87 GeV were carried out at the T1 line on the National Laboratory for High Energy Physics(KEK). Pions were produced from 8 GeV protons impinging on a beryllium internal target. Bending and focusing magnets directed these beams to a lead slit. The desired beam passed through the slit was once more bended in order to reduce the background due to neutral particles and led to the targets. Beam purity with respect to pions and noninteracting muons and electrons was measured by the use of a Cerenkov counter, and 90% for π^- at 0.87 GeV.

The targets were 40 mm diam metallic bismuth disks. The thickness is 4.0 g cm^{-2}. The particle fluence was determined by the two element (12) scintillator telescope, which is the same diam as the targets, in front of the targets. Beam intensity was about 2×10^4 sec^{-1} for π^- at 0.87 GeV. Pion exposure durations were from ten minutes to a few days in length to emphasize the production of residual radioactivities of varying half life. During the longer irradiations, temporal variations in the beam intensity were recorded and taken into consideration for the saturation values of the various activities. For the nuclides of the shorter half life, some tens of the shorter term exposures were repeated with the use of a pneumatic transport system and counts were accumulated to improve statistics.

Table I. Relevant Nuclear Properties of Measured Nuclides.[12]

Nuclide	Half life	Radiation in keV	Abundance	Nuclide	Half life	Radiation in keV	Abundance
^{206}Bi	6.24 d	803.	0.989	^{195}Hg^g	9.5 h	61.	0.908
^{205}Bi	15.3 d	1764.	0.325	^{193}Hg^m	11.1 h	258.	0.698
^{204}Bi	11.2 h	984.	0.572	^{199}Au	3.13 d	158.	0.394
^{203}Bi	11.8 h	820.	0.296	^{198}Au^m	2.27 d	215.	0.787
^{201}Bi^g	1.8 h	629.	1.00*	^{198}Au^g	2.70 d	412.	0.947
^{204}Pb^m	66.9 m	912.	0.965	^{196}Au^g	6.18 d	356.	0.88
^{203}Pb	52.1 h	279.	0.81	^{194}Au	39.5 h	329.	0.5913
^{201}Pb	9.4 h	331.	0.791	^{193}Au	15.8 h	186.	0.100
^{200}Pb	21.5 h	148.	0.284	^{165}Tm	29.6 h	243.	0.368
^{199}Pb	90. m	367.	0.648	^{161}Er	3.24 h	827.	0.609
^{198}Pb	2.4 h	173.	0.28	^{160}Er	29.4 h	729.	0.50
^{195}Pb	17. m	384.	0.894	^{160}Ho^m	5. h	729.	0.50
^{202}Tl	12. d	440.	1.00	^{157}Dy	8.1 h	326.	0.95
^{200}Tl	26.1 h	1206.	0.307	^{155}Dy	10.2 h	227.	0.652
^{199}Tl	7.4 h	455.	0.136	^{152}Dy	2.38 h	257.	1.00*
^{198}Tl^m	1.87 h	587.	0.520	^{152}Tb	17.5 h	344.	0.69
^{198}Tl^g	5.3 h	676.	0.108	^{139}Nd^m	5.5 h	738.	1.00
^{194}Tl^m	32.8 m	749.	1.00	^{113}Ag	5.3 h	298.	0.0824
^{203}Hg	46.8 d	279.	0.815	^{99}Mo	66.7 h	141.	0.95
^{199}Hg^m	42.6 m	158.	0.584	^{91}Sr	9.75 h	556.	0.615
^{195}Hg^m	40. h	262.	0.44				

* Assumed abundance.

All countings were done with a Ge(Li) detector system in a low-background environment. Induced radioactvitities in the targets were counted directly and after the radiochemical separations.[11] The γ-rays of interest in the spectra were summarized in Table I together with nuclear data used in the analysis of the experimental data.[12] The photo peak efficiencies of the detector was determined with the known radioactive source distributed homogeneously in a sample as same as the targets. The chemical yields were determined by a neutron activation method after the measurements of radioactivities at the Kyoto University reactor.

III. RESULT AND DISCUSSION

The absolute production cross sections of the residual products from the interactions of 0.87 GeV π^- with Bi are given in Table II. The uncertainties listed for the experimental data arise predominantly from determination of the photo peak intensities, and smaller contrbutions arise from corrections for photon absorption in the target, photo peak efficiency of the detector and variations in beam intensity during the irradiation. They do not include possible systematic uncertainties in γ-ray abundances. In the following

Table II. Summary of Measured Cross Sections.

Nuclide	Yield type*	Cross section in mb	Detection method[†]	Nuclide	Yield type*	Cross section in mb	Detection method[†]
^{206}Bi	I	76.9± 4.7	Ge	^{195}Hg^g	I	10.0± 3.7	Ge
^{205}Bi	I	114. ±11.	Ge	^{193}Hg^m	C	29.9± 7.2	Ge
^{204}Bi	I	36.3± 7.6	Ge	^{199}Au	I	<0.7	Ge
^{203}Bi	I	33.1±11.7	Ge	^{198}Au^m	I	<0.7	Ge
^{201}Bi^g	I	19.0± 3.6	Ge	^{198}Au^g	I	<0.4	Ge
^{204}Pb^m	I	24.9± 2.4	Ge	^{196}Au^g	I	<1.1	Ge
^{203}Pb	I	63.8±10.2	Ge	^{194}Au	I	6.4± 1.7	Ge
^{201}Pb	C	67.9± 5.8	Ge	^{193}Au	C′	37.1± 8.0	Ge
^{200}Pb	C	68.7±11.1	Ge	^{165}Tm	C	6.7± 1.2	Chem
^{199}Pb	C	66.9± 3.5	Ge	^{161}Er	C	6.7± 1.1	Chem
^{198}Pb	C	45.4±18.4	Ge	^{160}Er	C	4.1± 1.1	Chem
^{195}Pb	C	17.1± 6.5	Ge	^{160}Ho^m	C′	2.7± 0.7	Chem
^{202}Tl	I	16.5± 2.5	Ge	^{157}Dy	C	4.8± 0.4	Chem
^{200}Tl	I	21.5± 5.0	Ge	^{155}Dy	C	3.7± 0.4	Chem
^{199}Tl	I	29.0±13.6	Ge	^{152}Dy	C	2.0± 0.6	Chem
^{198}Tl^m	C	35.2± 5.0	Ge	^{152}Tb	C′	1.3± 0.5	Chem
^{198}Tl^g	C	29.0±13.6	Ge	^{139}Nd^m	I	0.7± 0.3	Chem
^{194}Tl^m	I	9.0± 2.1	Ge	^{113}Ag	C	2.2± 1.9	Chem
^{203}Hg	I	<1.6	Ge	^{99}Mo	C	4.2± 0.9	Chem
^{199}Hg^m	I	<2.3	Ge	^{91}Sr	C	1.5± 0.6	Chem
^{195}Hg^m	I	15.4± 5.1	Ge				

* The symbols used in this column have the following meanings: "I" is the independent yields; "C" is the cumulative yields; "C′" is the almost cumulative yields.

† The symbols used in this column have the following meanings: "Ge" is the direct γ-ray spectroscopy; "Chem" is the γ-ray spectroscopy after the radiochemical separations.

sections, we will discuss the interactions in three mass regions.

1. Near target mass region

In the near target mass region, attention should be called to the contributions of the secondary particles to the measured yields. Unfortunately, we could not estimate the effects of the secondary particles such as fast neutrons. Since most of the secondary particles have energies less than a few ten MeV,[13] however, they are expected to affect hardly the yields in the mass region $A < 203$.

For the first approximation of charge dispersion curve, we obtained a curve for $A = 202$, 203, having the full width at half maximum $\Delta Z = 1.60$ (Fig. 1). Assuming the same charge dispersion curve in the near target mass region, the cross section contour map was obtained as shown in Fig. 2.

Figure 2 shows a smooth trend of the production cross section, decreasing as the product mass decreases. In the mass region $A > 200$, the difference $(Z_p - Z_A)$ between the most probable charge Z_p and the position of β-stability[14] increases as the product
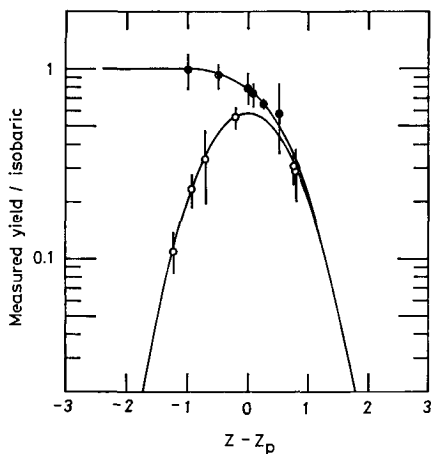
Fig. 1. Charge dispersion of products, in the near target mass region, produced by interaction of 0.87 GeV $\pi^- +$ Bi. Filled points indicate the cumulative yields and open points the independent yields.

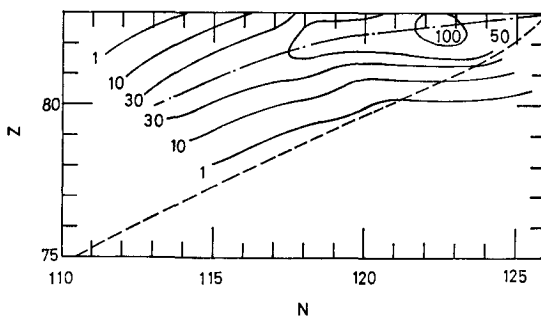Fig. 2. Cross section contour map in millibarn of 0.87 GeV $\pi^- +$ Bi. Dot-dash curve goes through the position of the most probable charge Z_p; dashed curve the position of β-stability Z_A.[14]
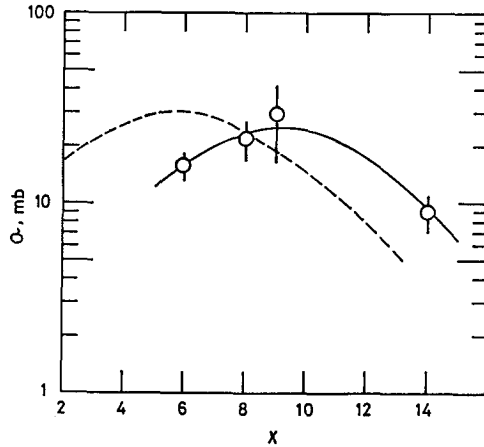
Fig. 3. Yields of ^{209}Bi (π^-, pxn) at 0.87 GeV. The numbers on the abscissa indicate those of emitted neutrons. Open points represent the measured independent yields. Solid curve is drawn to aid the eye. Dashed curve, which is arbitrary on ordinate, is taken from the stopped π^- experiment.[15]

mass decreases. In the mass region $A<200$, on the other hand, (Z_p-Z_A) is almost constant ($\sim$2.5) irrespective of the product mass. This fact probably indicates that the excitation energies of the spallation products do not depend on the product mass sensitively.

Figure 3 shows a comparison of reaction yields from ^{209}Bi (π^-, pxn) with 0.87 GeV π^- and stopped π^-.[15] The mean numbers of emitted neutrons are $\sim$9 and $\sim$7 for 0.87 GeV π^- and stopped π^-, respectively. This difference is probably attributed to the different momenta of the incident pions.

2. Deep spallation mass region

As shown in Table II, the number of the measured isotopes is not many enough to construct the charge dispersion curve in the mass region $A\sim$160. However, the values $(Z-Z_A)$ of the measured isotopes are very small compared to (Z_p-Z_A) of 2.5 which has been mentioned above. It can concludes, therefore, that the measured cumulative yields nearly equal to the total isobaric yields. Regarding the measured cumulative yields as the total isobaric ones, the mass yield curve was constructed as shown in Fig. 4.

The results of Monte Calro intranuclear cascade and evaporation calculation are also shown in Fig. 4.[16] 1,000 cascades were followed and errors quoted are statistical. From a comparison between the experimental and the predicted results, it is clear that the prediction overstimates the production cross sections in the deep spallation mass region and that it underestimated in the near target mass region.

The slope of the mass-yield curve for 0.87 GeV π^- + Bi is estimated to be 7%/amu in Fig. 4 and is compared with those of Cu spallation induced with pions, protons, and heavy ions[7] in Fig. 5. The pion results are plotted at an energy corresponding to the sum of their kinetic energy and the pion rest mass energy. It is interesting that the slope for Bi + π^- is nearer to the of protons and heavy ions rather than to that of pions.
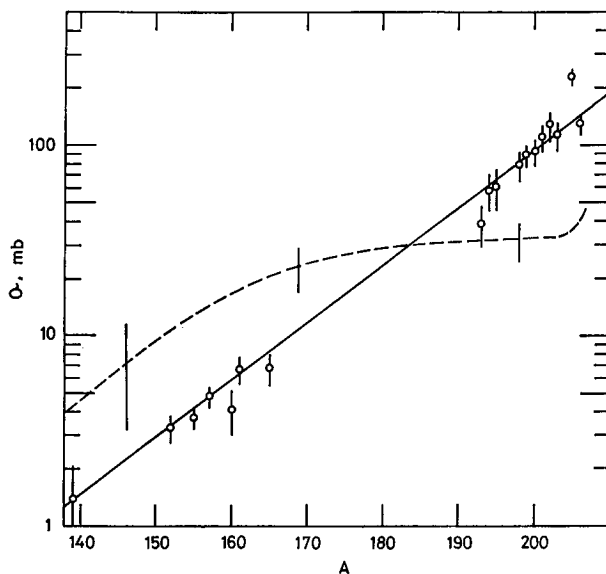
Fig. 4. Mass yield curve for 0. 87 GeV π⁻ induced spallation of Bi. Solid curve is drawn to aid the eye. Dashed curve goes through the calculated points.[16]
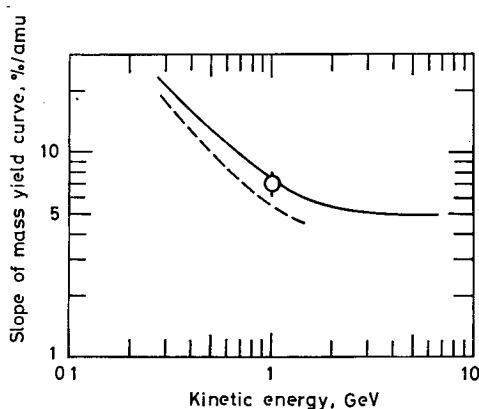

Fig. 5. Slope of the mass yield curve for spallation as a function of incident particle kinetic energy. Open point represents the result of 0. 87 GeV π⁻+Bi. Solid curve for Cu+ proton or heavy ion and dashed curve for Cu+π⁻ are taken from Ref.[7] The pion points are plotted at an energy corresponding to the sum of their kinetic energy and the pion rest mass energy.

3. Binary fission mass region

The binary fission is a characteristic decay mode for the heavy nuclei. For neutron rich nuclides in the mass region $A\sim100$, the mode of formation might be described as low-energy fission. The mass yield curve in this region is shown in Fig. 6 regarding the measured yields of some isotopes as the total isobaric yields. The observed hump in the mass region $A\sim100$, is fairly attributed to the low-energy fission. For lack of better
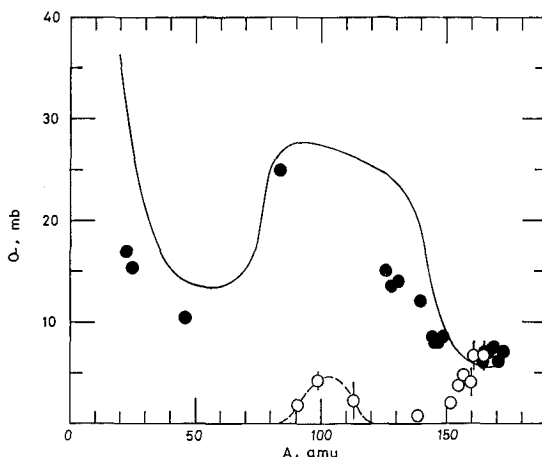
Fig. 6. Comparison of mass yield curves in the binary fission mass region. Open points represent the result of 0.87 GeV $\pi^- +$Bi. Filled points are the total isobaric yields for 28 GeV p+Th.[9] Solid curve goes through those for 28 GeV p+U.[8]

definition of the hump, one can assume the Gaussian distribution. This area amounts to ~100 mb or corresponds to a binary fission cross section of ~50 mb.

Figure 6 shows a compariton of mass yield curves in this region. The mass yield curves of 28 GeV proton induced reactions in U and Th are taken from Ref.[8,9] The neutron rich cumulative yields decrease in the order of U, Th, and Bi. This trend can be explained by the fissionabilities decreasing as the target mass decreases. However, the estimated binary fission cross section of ~50 mb is considerable small when compared to that measured by mica tachnique for 1 GeV p+Bi.[10] This difference is not known in any detail, but suggests further studies on the charge dispersion curve in this region.

IV. CONCLUSION

Some conclusions can be drawn in the present study of 0.87 GeV $\pi^- +$Bi:
(1) general trends of pion spallation in heavy target such as the slope or the mass yield curve show a good accordance with those of proton;
(2) when compared to the prediction of the intranuclear cascade and evaporation, however, some discordance is observed;
(3) furthermore, the estimated binary fission cross section is considerably lower than that reported for 1 GeV p+Bi.

ACKNOWLEDGEMENT

professors M. Honda, S. Tanaka (University of Tokyo) and H. Nakahara (Tokyo Metropolitan University).

REFERENCES

(1) P. L. Reeder and S. S. Markowitz, *Phys. Rev.*, **133**, B639(1964).

(2) D. T. Chivers, E. M. Rimmer, B. W. Allardyce, R. C. Witcomb, J. J. Domingo, and N. W. Tanner, *Nucl. Phys.*, **A126**, 129(1969).

(3) C. K. Garrett and A. L. Turkevich, *Phys. Rev.*, **C8**, 594(1973).

(4) H. E. Jackson, L. Meyer-Schutzmeister, T. P. Wangler, R. P. Redeverrie, R. E. Segel, J. Tonn, and J. P. Schiffer, *Phys. Rev. Lett.*, **31**, 1353(1973).

(5) N. P. Jakob, Jr. and S. S. Markowitz, *Phys. Rev.*, **C13**, 754(1976).

(6) C. J. Orth, B. J. Dropesky, R. A. Williams, G. C. Giesler, and J. Hudis, *Phys. Rev.*, **C18**, 1426(1979).

(7) P. E. Haustein and T. J. Ruth, *Phys. Rev.*, **C18**, 2241(1978).

(8) Y. Y. Chu, E. M. Frantz, G. Friedlander, and P. J. Carol. *Phys. Rev.*, **C4**, 2202(1971).

(9) Y. Y. Chu, E. M. Frantz, G. Friedlander, and P. J. Carol, *Phys. Rev.*, **C14**, 1068(1976).

(10) J. Hudis and S. Katcoff, *Phys. Rev.*, **C13**, 1961(1976).

(11) J. Klelinberg, Los Alamos Sci. Lab. Report No. LA-1721(1967).

(12) W. W. Bowman and K. W. Macmurdo, *Atomic Data and Nuclear Data Tables*, **13**, No. 2 and 3(1974) ; C. M. Lederer and V. S. Shirley, "Tables of Isotopes", Wiley-Interscience, New York (1978).

(13) S. Matsuki, T. Higo, Y. Iwashita, T. Yanabu, H. Itoh, T. Maki, A. Yoshimura, H. Yoshinaga, T. Cho, and S. Uehara, *Phys. Lett.*, **84B**, 67(1979).

(14) G. T. Garvey, W. J. Gerace, R. L. Jaffe, I. Talmi, and I. Kelson, *Rev. Mod. Phys.*, **41**, S1, (1969).

(15) H. S. Pruys, R. Engfer, R. Hartmann, U. Sennhauser, H. J. Pfeiffer, H. K. Walter, J. Morgenstein, A. Wyttenbach, E. Gadioli, and E. Gadioli-Erba, *Nucl. Phys.*, **A316**, 365(1979).

(16) H.W. Bertini, *Phys. Rev.*, **C6**, 631(1972) ; H. W. Bertini, M. P. Guthrie, and O. W. Hermann, Oak Ridge National Lab. Report No. ORNL-4564(1973).